

Supporting Information

# **A Multidentate Polymer Microreactor Route for Green Massive Fabrication of Mesoporous NaYF<sub>4</sub>**

Yameng Li,<sup>a, b</sup> Xiaozeng Zhang,<sup>a, b</sup> Zhicong Chao,<sup>a, b</sup> Minglong Gan,<sup>a, b</sup> Jinsheng Liao,<sup>a, b</sup> Xinyu Ye,<sup>a, c</sup> Weixiong You,<sup>a, c</sup> Junxiang Fu,<sup>\*a, b</sup> Herui Wen,<sup>\*a, b</sup>

Faculty of Materials Metallurgy and Chemistry, Jiangxi University of Science and Technology, Ganzhou, 341000, PR China E-mail: [brxw@qq.com](mailto:brxw@qq.com), [wenherui63@163.com](mailto:wenherui63@163.com)

Jiangxi Provincial Key Laboratory of Functional Molecular Materials Chemistry, Ganzhou, 341000, PR China

Key Laboratory of Rare Earth Luminescence Materials and Devices of Jiangxi Province, Ganzhou, 341000, PR China

\* To whom correspondence should be addressed. E-mail: [brxw@qq.com](mailto:brxw@qq.com) or [wenherui63@163.com](mailto:wenherui63@163.com)

## Experimental Section:

Liquid phase reaction: Mesoporous NaYF<sub>4</sub>: Yb, Er UCNPs were prepared by hydrothermal method using 9.19 g Y (NO<sub>3</sub>)<sub>3</sub>•6H<sub>2</sub>O, 2.52 g Yb (NO<sub>3</sub>)<sub>3</sub>•6H<sub>2</sub>O and 0.28 g Er (NO<sub>3</sub>)<sub>3</sub>•6H<sub>2</sub>O as raw materials. These starting materials were dissolved in 30 mL 50% PAAS solution to form A, 4.44 g NH<sub>4</sub>F was added to A and stirred for 1 h to get B, then B was put into the reaction kettle and maintained at 200 °C for 4 h. After the reaction, the hydrothermal kettle was naturally cooled to room temperature. All the precipitate was collected by centrifugation after washed with distilled water and pure ethanol for several times, and then drying in vacuum at 60 °C for 12 h.

Solid phase reaction: After the above process, the samples were annealed in a muffle furnace at 400 °C for 2 h under air atmosphere. Next, the calcined samples were obtained after cooling.

The crystal structure of as-prepared samples was obtained by Bruker D8 powder diffractometer with Cu K $\alpha$  radiation, and the XRD patterns were scanned in steps of 20°/min, from 20 to 80°, about 4 min per sample. The surface morphology was determined by scanning electron microscopy (SEM) (S-4800) on operating voltage at 1.5 kV. The specific surface and pore diameter distribution of sample microsphere structure was calculated by the Brunauer-Emmett-Teller (BET) measure of nitrogen adsorption-desorption analysis (V-Sorb 4800P). The process of degradation was followed by analysis on a UV spectrophotometer (UV-2550) to monitor the concentration of the residual dyes at their characteristic wavelength (MB-664 nm). The chemical composition of samples was characterized by an infrared spectrometer (Bio-Rad FTS-3000). In order to determine the heating temperature needed to thoroughly remove PAAS, the thermal behavior of samples was declared with differential thermal analysis (DTA) and thermal gravimetric analysis (TGA) within a temperature range of 20~800 °C with a heating rate of 10 °C /min. The UC spectra were obtained using a SENS-9000 spectrophotometer (Zolix, China) equipped with an external 980 nm diode laser.

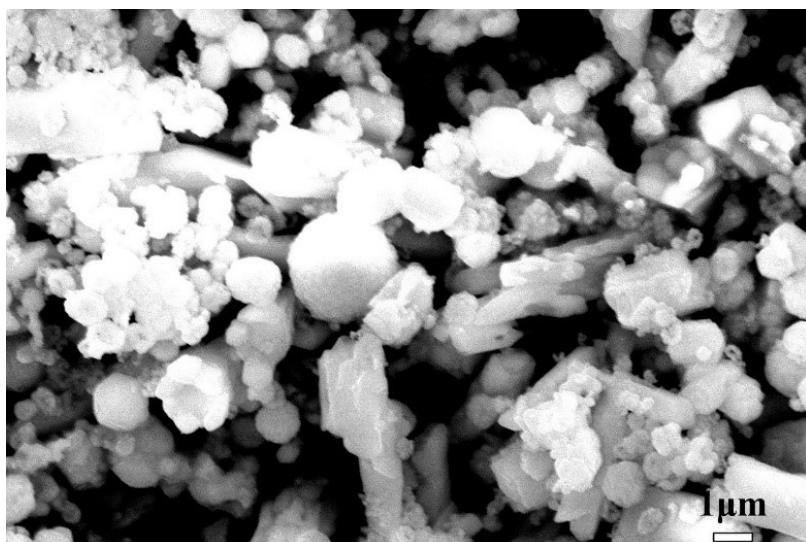


Fig. S1 SEM image of the product using sodium acrylate as ligand.

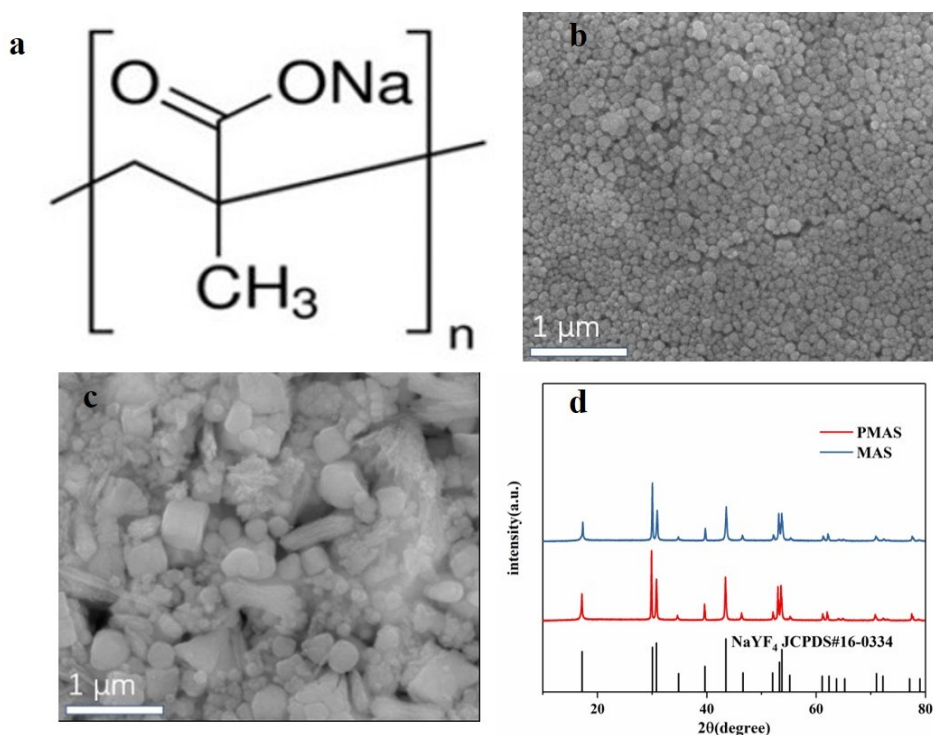


Fig. S2 The structural simplification of sodium polymethacrylate (PMAS) (a); The SEM images of the final products using different ligands as multidentate polymer microreactor: (b) PMAS; (c) sodium methacrylate (MAS); (d) The XRD patterns of these two samples.

Compared with PAAS, PMAS has an additional methyl group in each repeat unit (Fig. S2a). At the same experimental conditions, with  $\text{NH}_4\text{F}$  as fluorine source, the final product is 100nm uniform  $\text{NaYF}_4$  nanocluster (Fig. S2b). So, we suppose other polymers with  $-\text{COO}^-$  groups should have similar multidentate polymer microreactor effect.

In addition, we use PMA monomer as control group, and the final product is a mixture of irregular spheres, rods and chaotic flocs, totally different from PMAS (Fig. S2c). This result confirms that the presence of the multidentate polymer chain structure is essential for the formation of nanoclusters.

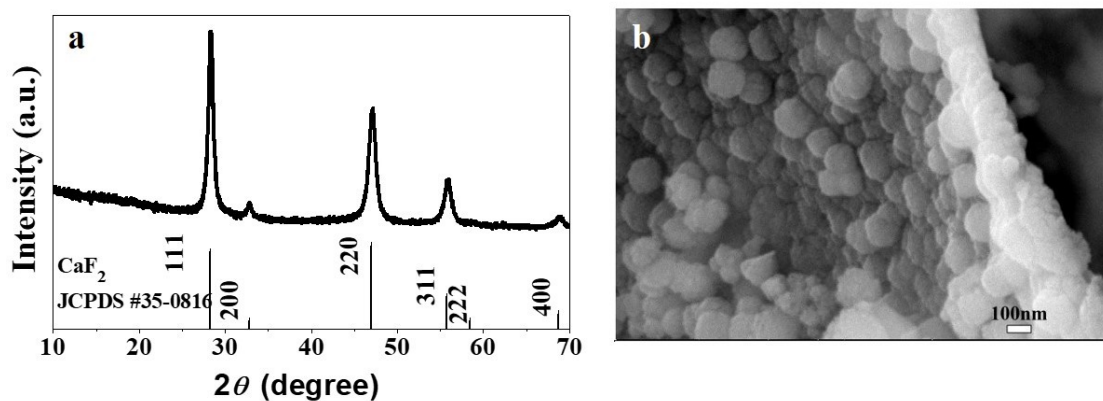


Fig. S3. (a) The XRD patterns of the CaF<sub>2</sub>: Yb, Er. (b) SEM images of the morphology of CaF<sub>2</sub>: Yb, Er.

We find CaF<sub>2</sub> can also be prepared via this multidentate polymer microreactor route, which confirms the universality of this multidentate polymer microreactor method (Fig. S3, ESI<sup>†</sup>). The XRD pattern in Fig. S3a indicates that all diffraction peaks of the product can be matched well with the standard data of CaF<sub>2</sub> (JCPDS#35-0816). Based on the XRD spectra and Scherer's formula, the average grain size of the CaF<sub>2</sub> product is 17.2 nm. Fig. S3b shows the SEM image of CaF<sub>2</sub> sample. The size of rough spherical clusters is about 100 nm.

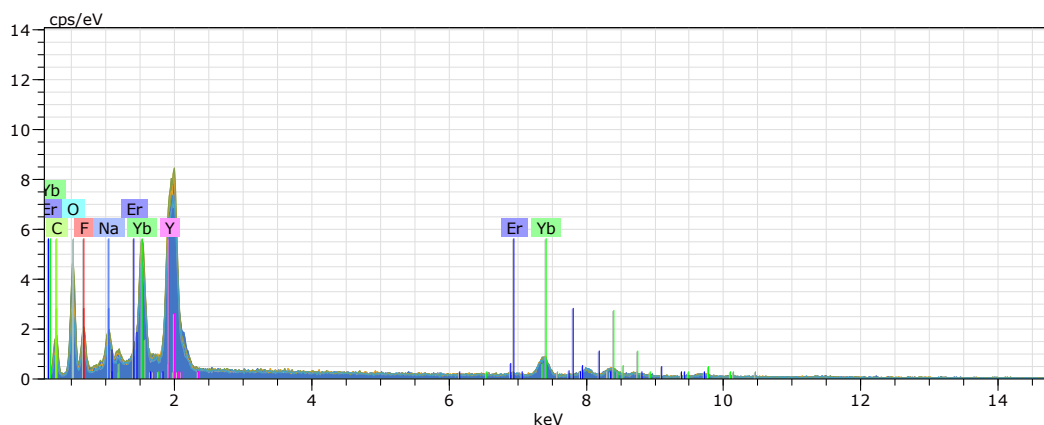


Fig. S4 EDS patterns of as-prepared clusters via different fluoride sources: (a)  $\text{NH}_4\text{F}$ ; (b)  $\text{NH}_4\text{F}$ :  $\text{NaF}$ ; (c)  $\text{NaF}$ .

Table S1. EDS content of as-prepared clusters via different fluoride sources: (a)  $\text{NH}_4\text{F}$ ; (b)  $\text{NH}_4\text{F}$ :  $\text{NaF}$ ; (c)  $\text{NaF}$ .

Element	$\text{NH}_4\text{F}$	$\text{NH}_4\text{F}$ : $\text{NaF}$	$\text{NaF}$	Theoretical value
<b>F</b>	65.36	64.28	67.63	□
<b>Na</b>	13.78	11.98	10.55	□
<b>Y</b>	15.7	18.53	16.7	□
<b>Yb</b>	4.79	4.81	4.64	□
<b>Er</b>	0.37	0.4	0.48	□
<b>Y/Ln</b>	75%	78%	77%	78%
<b>Yb/Ln</b>	23%	20%	21%	20%
<b>Er/Ln</b>	1.8%	1.7%	2.2%	2%

We carefully examine the EDS of as-prepared clusters of three sizes to find that the actual doped Yb/Er values close to the theoretical doping amount and there is no significant difference among them. We suppose the different luminescence intensity of  $\text{NaYF}_4$ : Yb, Er of three sizes may due to crystallinity and surface defects.  $\text{NH}_4\text{F}$  has a much larger solubility than  $\text{NaF}$ , and more  $\text{F}^-$  in the solution could lead to better crystallinity and less surface defects which further results in better luminescence intensity.

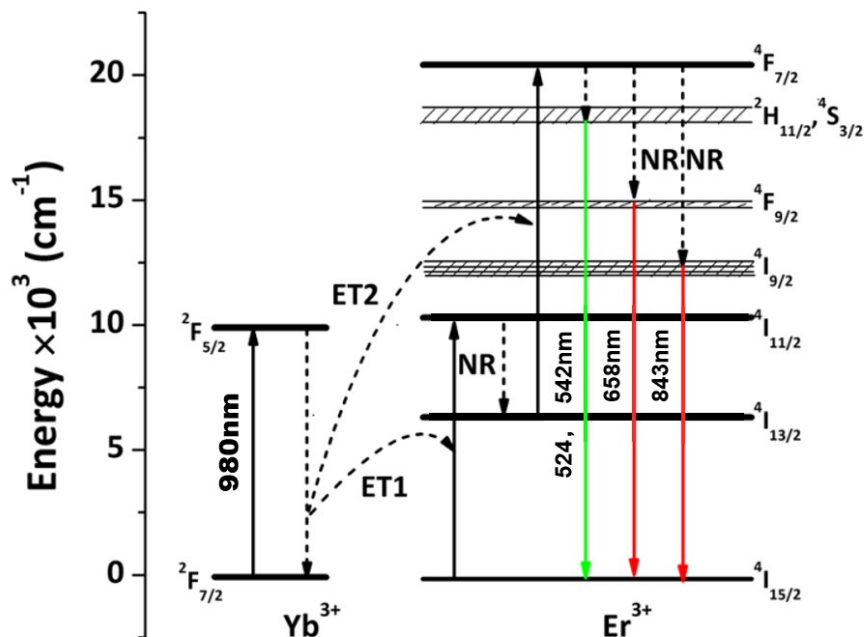


Fig. S5 A schematic illustration of the energy levels and UC processes for mesoporous NaYF<sub>4</sub>: Yb, Er microspheres.

Our upconversion luminescence spectra shows NaYF<sub>4</sub>: Yb, Er clusters using NaF as fluoride sources have larger size and stronger the relative intensity at 843 nm. The photon reactions of the 843 nm UC process can be presented as  ${}^4I_{9/2} \rightarrow {}^4I_{15/2} + h\nu$ . Therefore, we suppose NaYF<sub>4</sub>: Yb, Er clusters using NaF as fluoride sources tend to promote relaxation process of  ${}^4F_{7/2} \rightarrow {}^4I_{9/2}$  other than  ${}^4F_{7/2} \rightarrow {}^2H_{11/2}$ ,  ${}^4F_{7/2} \rightarrow {}^4S_{3/2}$  or  ${}^4F_{7/2} \rightarrow {}^4F_{9/2}$  and raise the population of  ${}^4I_{9/2}$  state.

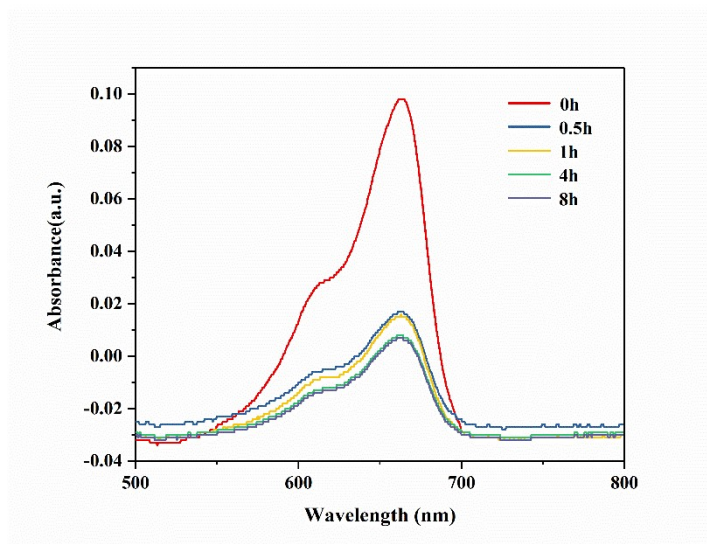


Fig. S6 UV-vis adsorption spectra of methylene blue solution with mesoporous NaYF<sub>4</sub>: Yb, Er microspheres.

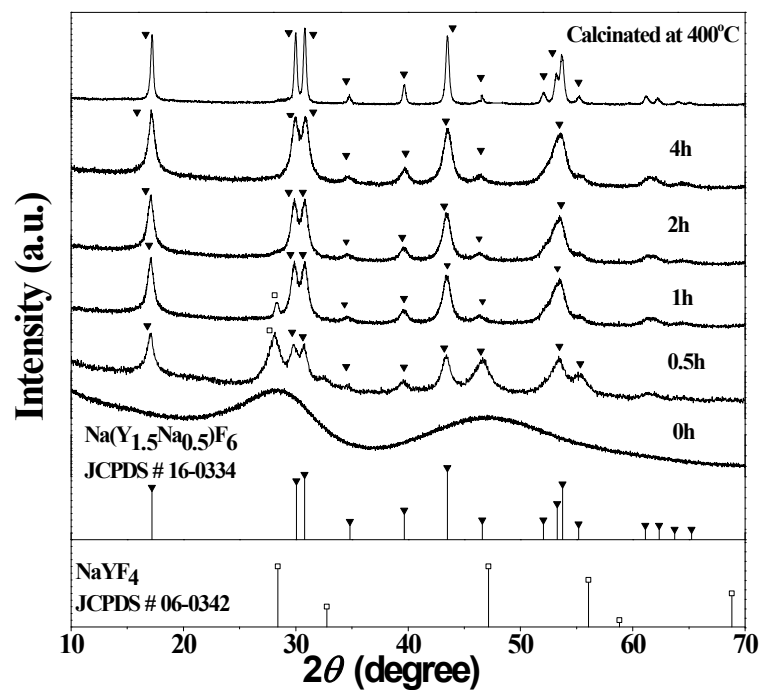


Fig. S7 XRD patterns of the MPUCS fabricated at 220 °C for 0, 0.5, 1, 2, 4 h and the sample (220 °C, 4 h) calcined at 400 °C for 2 h.

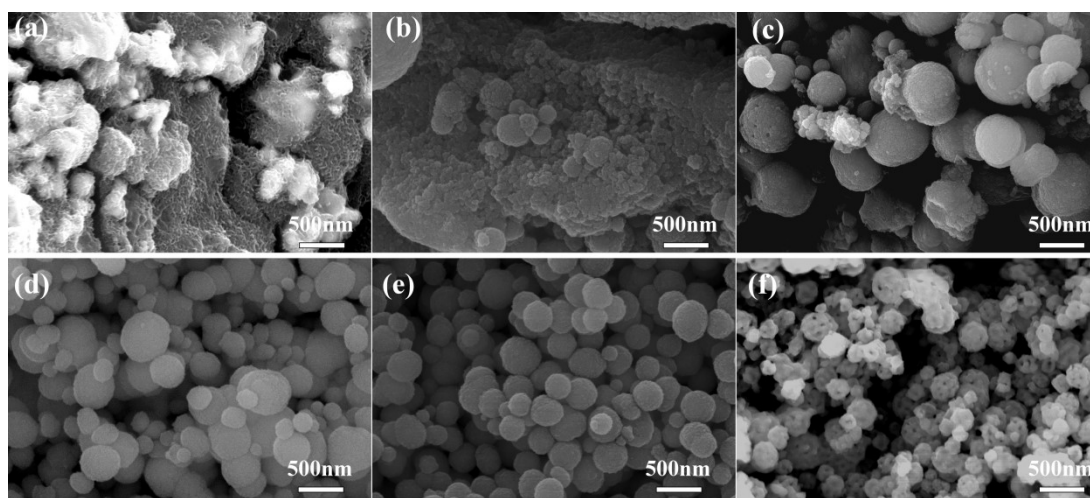


Fig. S8 SEM images of the MPUCS fabricated at 220 °C for (a) 0 h, (b) 0.5 h, (c) 1 h, (d) 2 h, (e) 4 h, (e) calcined at 400 °C for (f) 2 h.

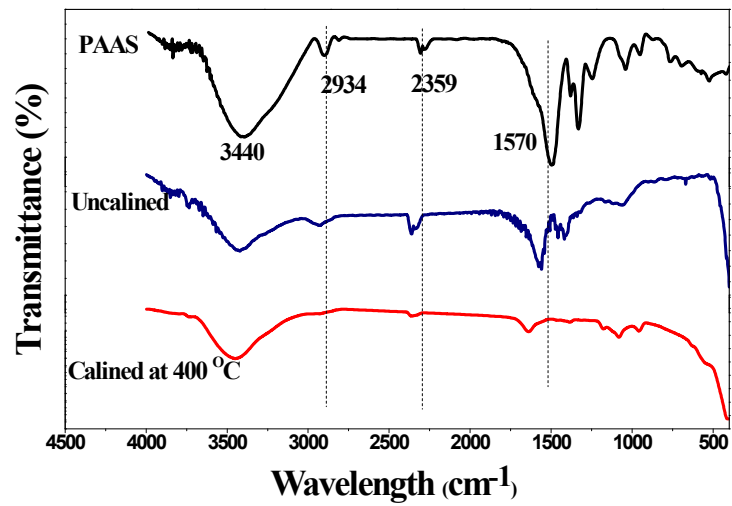


Fig. S9 FT-IR spectrum for PAAS raw material, mesoporous  $\text{NaYF}_4$ : Yb, Er microspheres and mesoporous  $\text{NaYF}_4$ : Yb, Er microspheres calcined at  $400^\circ\text{C}$  for 2 h.

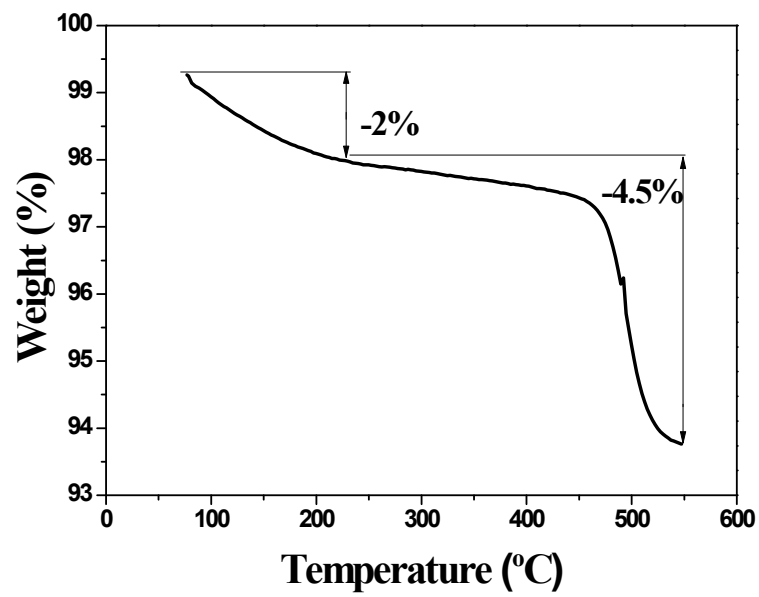


Fig. S10 TGA curve of mesoporous  $\text{NaYF}_4$ : Yb, Er microspheres.



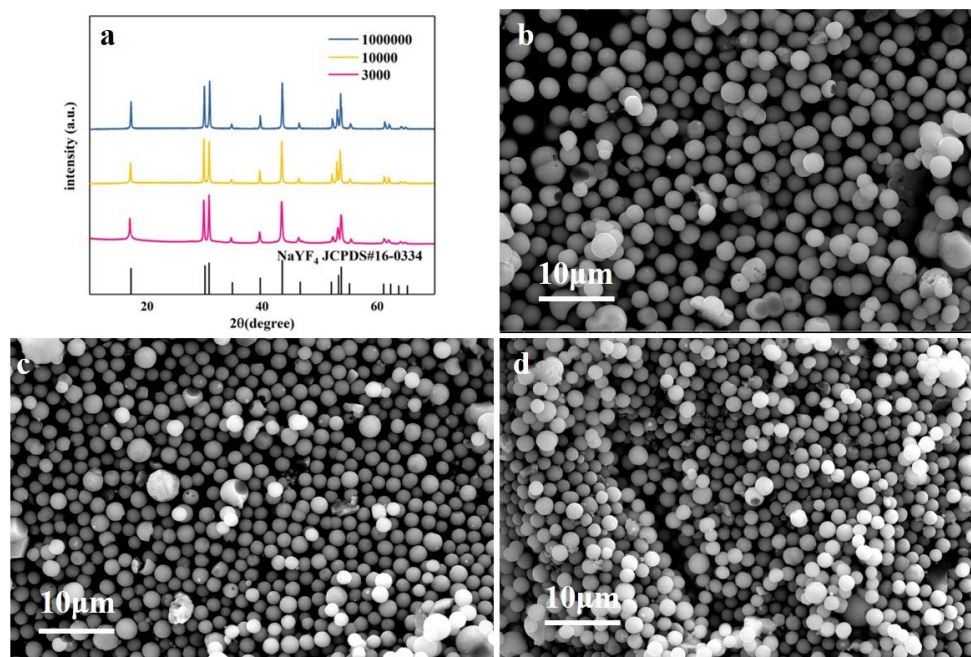


Fig. S11 (a)XRD patterns and (b-d) SEM images of NaYF<sub>4</sub>: Yb, Er samples at different molecular weight varies from 3000, 10000 to 1,000,000.

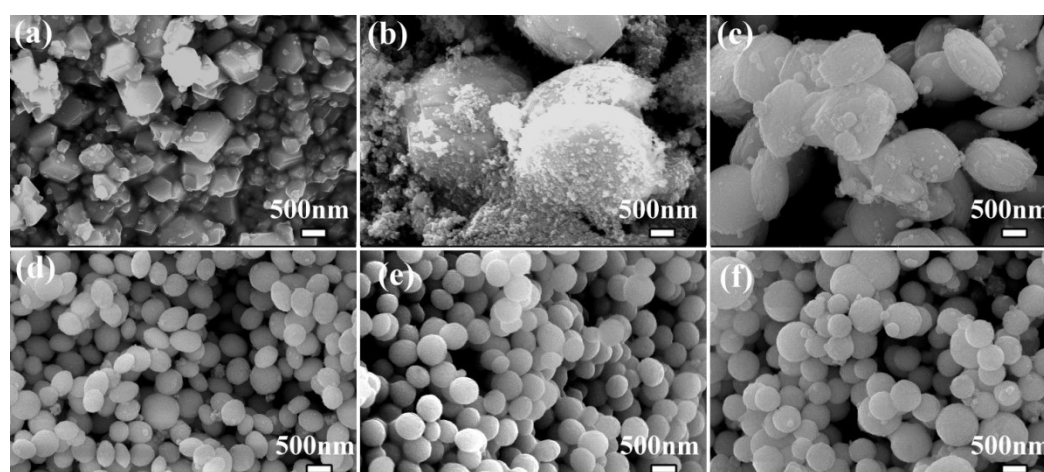


Fig. S12 SEM images of the samples fabricated at different mass percentage of PAAS solution (a) 0, (b) 10%, (c) 20%, (d) 30%, (e) 40% and (f) 50%.

Fig. S12 shows the SEM images of the hydrothermal samples at different mass percentage of PAAS aqueous solution. With the absence of PAAS, it is found that the shape of the obtained sample is bulk-like microstructure. When the mass percentage of PAAS increases to 10%, the nanoparticle gradually appears on the surface of the sample. As the mass percentage of PAAS further increases to 20%, the large oval particles change into small oval particles. When the mass percentage of PAAS reaches 30%, uniform spherical particles can be obtained. Further increase the mass percentage of PAAS to 50%, the sample remains spherical particles, which indicates that the suitable mass percentage range of PAAS synthesized spherical particles is 30%-50%. In addition, it confirms that appropriate concentration of PAAS is necessary to the formation of mesoporous NaYF<sub>4</sub> clusters.